

See discussions, stats, and author profiles for this publication at: <https://www.researchgate.net/publication/334437387>

Design of a stiffness variable flexible coupling using magnetorheological elastomer for torsional vibration reduction

Article in *Journal of Intelligent Material Systems and Structures* · July 2019

DOI: 10.1177/1045389X19862378

CITATION

1

READS

330

3 authors, including:



Kanghyun Lee
Seoul National University

4 PUBLICATIONS 1 CITATION

[SEE PROFILE](#)



Young-Keun Kim
Handong Global University

50 PUBLICATIONS 211 CITATIONS

[SEE PROFILE](#)

Some of the authors of this publication are also working on these related projects:



US ONR Remote 6-DOF sensor [View project](#)



SLM process simulation [View project](#)

Design of a stiffness variable flexible coupling using magnetorheological elastomer for torsional vibration reduction

Journal of Intelligent Material Systems and Structures

1–10

© The Author(s) 2019

Article reuse guidelines:

sagepub.com/journals-permissions

DOI: [10.1177/1045389X19862378](https://doi.org/10.1177/1045389X19862378)

journals.sagepub.com/home/jim



Kang-Hyun Lee¹, Jae-Eun Park² and Young-Keun Kim² 

Abstract

In this study, the design of an magnetorheological elastomer flexible coupling whose torsional stiffness can be controlled by an embedded magnetic field generator is proposed. It is designed to minimize the torsional vibration transmission between shafts adaptively to the dynamic disturbance. The coupling insert is composed of magnetorheological elastomer which is a smart material whose stiffness can be controlled by an external magnetic field. This article also proposes a compact magnetic field generator which can be fitted inside the coupling hubs, to control the torsional stiffness of the magnetorheological elastomer. The finite element method was used to design and estimate the dynamic stiffness variation of the magnetorheological elastomer coupling due to the applied magnetic field and disturbance frequency. Also, torsional vibration experiments were conducted to validate the performance of the proposed magnetorheological elastomer coupling. Results showed that it can adaptively tune in a range of frequencies between 16.8 and 23.5 Hz and has 95.7% stiffness variation under magnetic field of 150mT. The proposed system is expected to achieve a higher MRE effect with a softer base matrix.

Keywords

magnetorheological (MR) effect, MRE module, smart material, stiffness control, torsional vibration, flexible coupling, magnetorheological elastomer

I. Introduction

Torsional vibration is a common concern in mechanical systems with rotating shafts for it can damage the mechanical elements of a system and cause noise that degrade the system performance. It can be caused by several factors such as torque fluctuation or shaft misalignment (DeSmidt et al., 2002; Steinel and Tebbe, 2004).

A flexible coupling is used to minimize the effect of the aforementioned shaft disturbance vibration and misalignment (Xu and Marangoni, 1994). It has a low stiffness that significantly reduces the natural frequency of the shaft below the normal operating speed to avoid the resonance problem. Torsional couplings are applied on the vehicle transmission or gearbox to aid in transmitting the torque smoothly and reduce the torsional vibration caused by fluctuating torque (Drexel, 1987; Kim, 2005). Also, it is applied on a powertrain system such as a diesel engine to damp the vibration of crank-shaft (Yamauchi et al., 1999).

However, a powertrain of vehicle is a complex system that has several different natural frequency for

each gear level (Hwang et al., 2000; Zhang et al., 2003). Thus, when a powertrain accelerates or decelerates, it can trigger one or several natural frequencies which amplifies the unwanted torsional vibration (Hoang et al., 2009). For such cases, a shaft coupling with a fixed stiffness is not able to adaptively damp out those wide band of excitations of disturbance. To adaptively tune the damper of a shaft for a wide band of torsional vibration, Hoang et al. (2010, 2013) proposed a dynamic absorbers with tunable stiffness based on a smart material of magnetorheological elastomer (MRE).

¹Department of Mechanical and Aerospace Engineering, Seoul National University, Seoul, Republic of Korea

²School of Mechanical and Control Engineering, Handong Global University, Pohang, Republic of Korea

Corresponding author:

Young-Keun Kim, School of Mechanical and Control Engineering, Handong Global University, Pohang 37554, Republic of Korea.
Email: ykkim@handong.edu

An MRE is a material whose stiffness and damping properties can be controlled by an external magnetic field (Carlson and Jolly, 2000; Stepanov et al., 2007; Zhou, 2003). An MRE-based vibration absorber system can work at a wider range of frequencies since its stiffness can be adaptively tuned to a varying excitation. Deng et al. (2006) designed an MRE-based vibration absorber that can be tuned from 55 to 82 Hz, which is a relative frequency change of 147%. Li et al. (2013) proposed an MRE-based seismic isolator that exhibits a change in lateral stiffness of up to 38% under a magnetic field of 0.3 T. Xin et al. (2017) proposed an MRE-based dynamic vibration absorber for powertrain mount systems which has tuning frequency range from 22.7 to 31.9 Hz with 40.5% relative change. Kim et al. (2011, 2012, 2017) and Shin et al. (2015) proposed an adaptive tunable vibration absorber (ATVA) using MRE to robustly suppress harmonic vibration of a miniature cryogenic cooler under varying disturbance. Jang et al. (2018) designed a compact MRE-based tunable vibration absorber (TVA) for easy installation which has 58% vibration suppression ability in the frequency range of 51.6 to 71.9 Hz. Also, there are other research on MRE isolators such as seismic vibration control for buildings (Yang et al., 2014), controlling negative stiffness using hybrid magnets (Yang et al., 2016) and combining MRE with MR fluid to control both stiffness and damping (Sun et al., 2017).

Almost all MRE-based vibration absorbers were designed for translational vibration such as compression or shear motion. In comparison, there have been relatively few studies of torsional vibration systems. Hashi et al. (2016) proposed a mathematical model of MRE for torsional vibration of a cylindrical MRE specimen. A torsional vibration with a disk-shaped absorber mass and MRE by Hoang et al. (2013) achieved a 53% stiffness tuning performance. But, this required an external frame to hold the electromagnet which made the whole system bulky.

Two main design criteria should be considered to apply a smart MRE-based torsional damper on an actual shaft system such as a powertrain of a vehicle, where energy is mainly distributed less than 30 Hz (Bai et al., 2017).

Since the target plant has restricted space constraints for additional installation, the MRE-based system including the magnetic field generator should be designed as compact as possible, without changing the design of target system. Also, the overall power consumption of the MRE-based damper is another important design issue. An electromagnet can generate a high magnetic field to control a wide stiffness of MRE, but it consumes a high power as much as 3 A, which can lead to heating problem and low energy efficiency for a long-term usage.

Therefore, this article proposes a novel compact MRE torsional damper in a form of a flexible coupling

with embedded magnetic field generator. Unlike previous MRE-based torsional vibration absorbers which has disk-shaped design, the proposed system is designed as a flexible coupling to easily attach and integrate on actual shaft system. Also, the proposed MRE coupling does not require to install additional device such as external electromagnet, which makes the system bulky, for it has a permanent magnet-based magnetic field generator inside the MRE coupling. It can generate as high as 150 mT by rotating the magnet with a small stepper motor, which does not consume additional power to maintain at a constant magnetic field level.

The article is structured as follows. The first section presents the design process of the MRE coupling and derives the system modeling. Then, the design process and simulation of the embedded magnetic field generator is described. The stiffness model of the proposed MRE coupling is derived based on the property test results and simulation results. Different simulation methods for the MRE coupling stiffness based on linear and non-linear spring models are proposed. Finally, the overall performance of the vibration suppression of the proposed system is analyzed and the the stiffness model is compared with experiment results.

2. Design and modeling of MRE coupling

2.1. Hardware design of the MRE coupling

This section describes the design process of a MRE coupling with controllable torsional stiffness that reduces disturbance passed between two shafts. A magnetic field generator with permanent magnets to control the MRE stiffness is also designed to be embedded in the coupling, to make the whole system to be compact and easily installable on an existing shaft applications.

The prototype of MRE coupling system is composed of three parts: MRE insert, coupling hubs with flanges and magnetic field generator. The overview of proposed system is shown in Figures 1 and 2.

The coupling hubs are designed as hollow cylindrical structure and the total length and diameter are 120 mm and 80 mm, respectively. To provide enough space to place the proposed magnetic field generator, the inner diameter is set as 65 mm. At ends of the coupling are designed as flanges with the diameter of 58 mm to connect with the shafts of diameter 17.5 mm. The coupling hubs are made of aluminum, which is non-ferromagnetic material to prevent from magnetic field interference.

The MRE insert is manufactured as two pieces of half hollow cylinder and they are placed in between the two coupling hubs as shown in Figure 1. The direction of the CIP is aligned along the direction of the magnetic field, and perpendicular to the torsion force. The MRE insert acts as the spring that generates elastic force under rotational or translational force applied

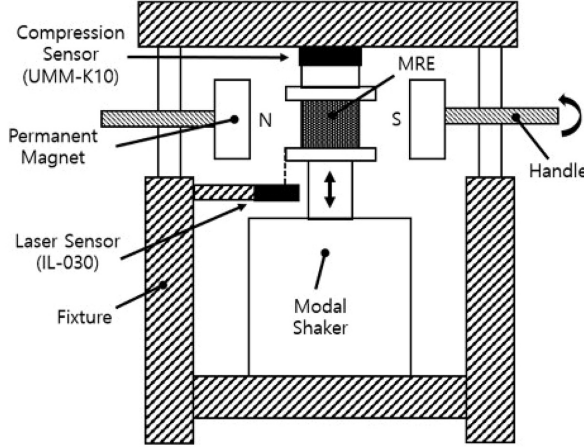


Figure 1. Proposed MRE coupling.

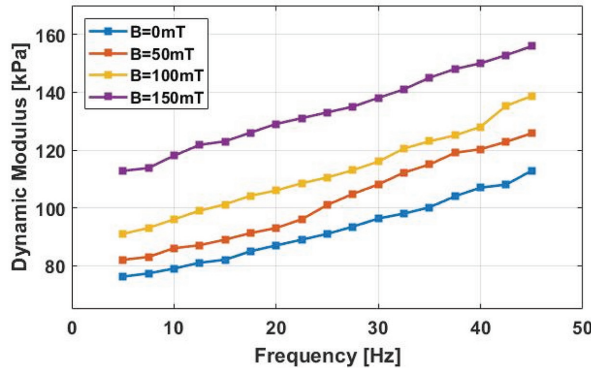


Figure 2. Cross-sectional view of MRE coupling.

onto the shaft. Depending on the magnitude of magnetic field, the stiffness of the MRE coupling is determined and the system can be modeled as a 1-DOF system.

2.2. System modeling

The MRE coupling is installed between two load shaft and the system can be modeled as a 1-DOF torsional vibration system as in Figure 3. One of the shafts transmits the vibrating torque ($T_{in}(t)$) to the other shaft that results output angular displacement (θ_{out}).

The dynamic equation of this system can be described as

$$J_o \ddot{\theta}_{out} + c_{MRE} \dot{\theta}_{out} + k_{MRE} \theta_{out} = T_{in}(t) \quad (1)$$

where $J_o(0.0018 \text{ kg} \cdot \text{m}^2)$ is the rotational inertia of the output load including the coupling hub mass, c_{MRE} is the damping constant, and k_{MRE} is the stiffness of the MRE. It is assumed that the shaft has too high stiffness and too low damping to be considered in the modeling.

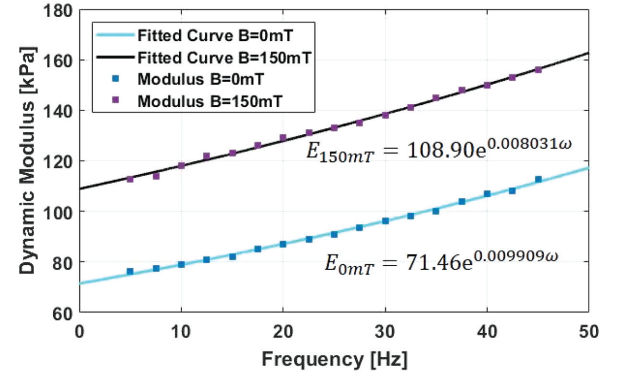


Figure 3. One-DOF torsional vibration system with MRE coupling.

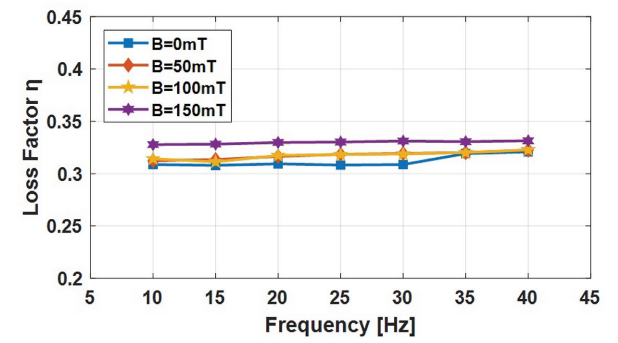


Figure 4. Interior features of MRE coupling.

The torsional displacement transmissibility (T_d) between the amplitudes of θ_{out} and θ_{in} is derived as follows

$$T_d = \frac{\theta_{out}}{\theta_{in}} = \left(\frac{k_{MRE}^2 + (c_{MRE}\omega)^2}{(k_{MRE} - J_o\omega^2)^2 + (c_{MRE}\omega)^2} \right)^{1/2} \quad (2)$$

3. Design and simulation of magnetic field generator

This study proposed a compact design of magnetic field generator which can be inserted inside the coupling hub, unlike other similar research that use external magnetic field generator to control the MRE stiffness. By inserting the magnetic field generator inside the coupling, it solves the limitation of requiring a large space externally for magnetic field control devices.

The proposed generator is as shown in Figure 4. Permanent magnets that can generate 150 mT are used for high power efficiency. Permanent magnets do not require additional power to generate a constant magnetic field, while an electromagnets requires continuous supply of electric current.

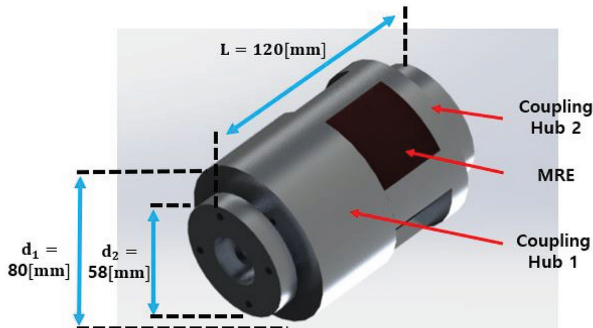


Figure 5. Simulation of the magnetic field generator using FEMM.

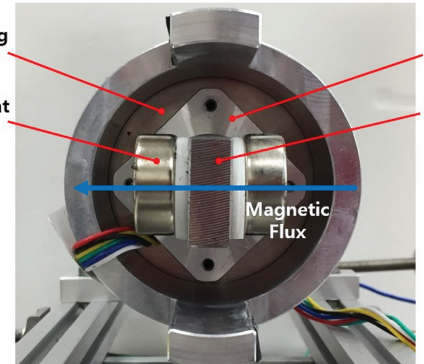


Figure 7. Experimental setup for measuring Young's modulus and loss factor of MRE.

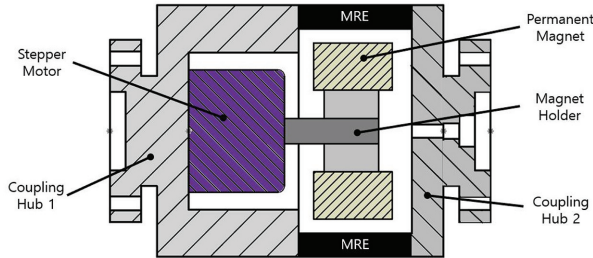


Figure 6. Relationship between the motor angle and magnetic field

The magnitude of magnetic field density on the MRE can be controlled from about 0 mT to 150 mT by rotating the magnet by a small stepper motor(NK243-01AT), as shown in Figure 4. Once the magnet is set at the required angular position, only a low current is consumed by the motor to maintain that magnetic field generation. The motor is a low powered one that has rated voltage of 6 V, rated current is 1.2 A, and the dimension of $42 \times 42 \times 34$ mm which is small enough to be fitted in the coupling hub.

The magnetic field applied on the MRE specimens by the proposed magnet system is analyzed by an electromagnetic simulation program(FEMM) as shown in Figure 5. The existence of MRE affects the path of magnetic flux density; thus, FEM modeling of MRE is needed to obtain the accurate simulation result. However, an accurate non-linear FEM model of MRE is too complex to be designed, thus the MRE, with a high percentage of iron particles aligned in chains, is assumed as ideal ferromagnetic material for simulation. The simulation results in Figure 5 show that the maximum magnetic field it can generate is about 148 mT when the magnet poles are aligned closest to the MRE specimen. The minimum magnetic field is about 0.35 mT when the magnet poles are farthest.

From this magnetic simulation, the relationship of the magnetic field generation with the angular position of the magnet is derived as in Figure 6, with a derived

equation as follows with adjusted R-square value of 0.9941

$$B(\theta) = -2.8970 \times 10^{-4}\theta^3 + 0.0428\theta^2 + 0.1282\theta + 0.5619 \quad (3)$$

4. MRE stiffness analysis and modeling

This section details the modeling of MRE stiffness based on the dynamic property test results. First, the dynamic properties of MRE for design of the proposed flexible coupling are conducted. Then, linear and non-linear stiffness modelings are derived.

4.1. Property test

The MRE specimen used in this study consists of a silicon base (Ecoflex 0010) and a carbonyl iron particle (CIP 3189, BASF) with ratio of 30 wt%. When an external magnetic field is applied to the MRE specimen, these iron particles tend to align as chain structures that consequently changes the material properties of the MRE, such as stiffness and damping. During the curation, it was hardened under a strong magnetic field of 500 mT to form CIP chains. The MRE sample is fabricated as cubes with a side length of 30 mm and experiments are conducted to analyze the dynamic modulus and loss factor of the MRE to be used for designing the MRE coupling.

The experiment setup is designed to conduct the dynamic compression testing to measure the the dynamic modulus and loss factor of the MRE. The experimental setup for compression test is built as shown in Figure 7. The compression force is perpendicular to the direction of magnetic field. The MRE sample is placed between the two permanent magnets and the direction of CIP chain of MRE specimen is same as the direction of magnetic field. The distance between the magnets can be adjustable by a handle and screws to control the applied magnetic field. The magnetic flux

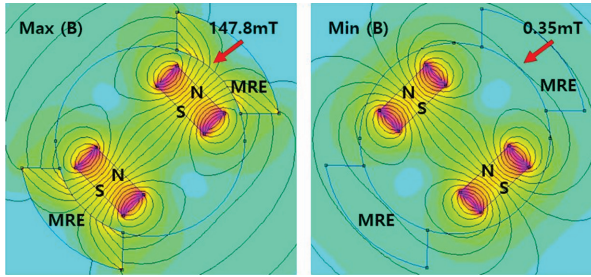


Figure 8. Dynamic modulus of MRE at varying excitation frequencies and magnetic flux densities.

density, the compression force, and the strain of the MRE sample are measured by a gaussmeter(MG3002, Lutron), compression load cell (UMM-K10, Dacell), and laser distance sensor (IL-030, Keyence), respectively. From the measurements, the Youngs modulus of the MRE can be derived from the following equation

$$E = \frac{FL}{\Delta A} = \frac{\sigma_0}{\varepsilon_0} (\cos\delta + i\sin\delta) = E' + iE'' \quad (4)$$

where E is the Young's modulus, F is the compression force applied, A is the initial cross-sectional area, L is the length of the sample, and ΔL is the change in length along the direction of the applied force. σ_0 is the stress amplitude, ε_0 is the strain amplitude, and δ is the loss angle. The loss factor (η) can be obtained by the loss angle as $\eta = \tan\delta$ and the damping ratio is then obtained as $\zeta = \frac{\eta}{2}$. Because the MRE is a silicon rubber-based viscoelastic, the modulus is divided into a real part of the storage modulus (E') and an imaginary part of the loss modulus(E'').

Dynamic modulus and the loss factor of MRE sample were measured at various excitation frequencies and magnetic flux densities. The frequency of the compression were varied from 5 to 45 Hz and the magnetic field were varied from 0 to 150 mT with a step of 50 mT. The results in Figure 8 show that the dynamic modulus increases as the excitation frequency increases. Also, the dynamic modulus showed to be increasing with the

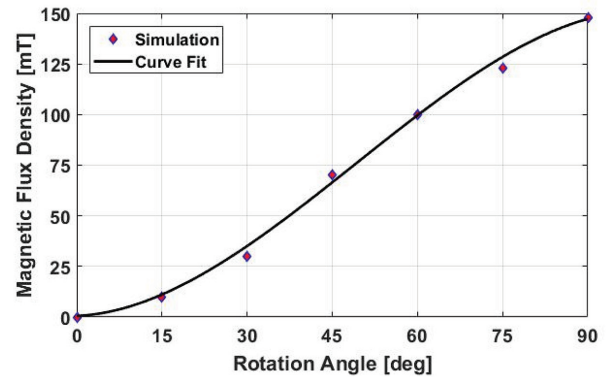


Figure 9. Maximum and minimum dynamic modulus and fitted curve when $B = 0$ mT, 150 mT (exponential).

magnetic flux density. The modeling of the storage modulus in terms of compression frequency under the magnetic field of 0 mT and 150 mT, which are the minimum and maximum of the applied magnetic field, are derived using exponential curve fitting as shown in Figure 9

$$E_{0mT} = 71.46e^{9.91 \times 10^{-3}\omega} \quad (5)$$

$$E_{150mT} = 108.90e^{8.03 \times 10^{-3}\omega} \quad (6)$$

Experimental results showed that the loss factor of the MRE is fairly constant that indicates that the excitation frequency and the magnetic flux density have little effect on the loss factor, as shown in Figure 10. In this study, the loss factor of the MRE is estimated as a constant value of $\eta = 0.3210$ and the system damping ratio is constant with the value of $\zeta = 0.1605$

4.2. MRE stiffness modeling

Based on the material property results, the modelings of MRE stiffness are derived to estimate the vibration transmissibility of the proposed system.

This article explains two different methods for estimating the stiffness of the MRE coupling in simulation.

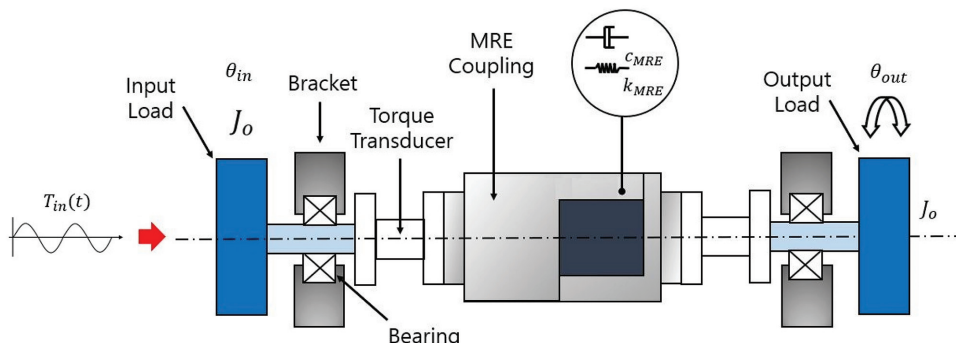


Figure 10. Loss factor of MRE at varying excitation frequencies and magnetic flux densities.

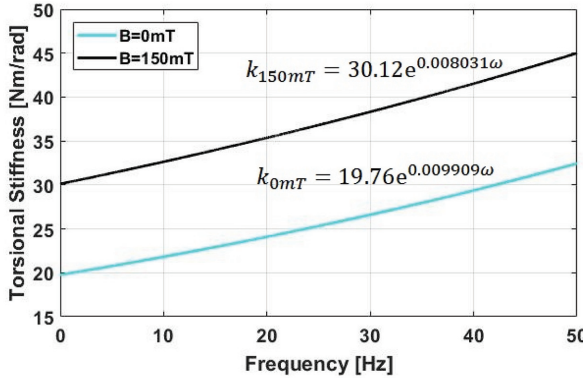


Figure 11. Torsional stiffness of MRE coupling (assuming linear translational spring).

The first method assumes the MRE as a linear elastic material and the second method assumes it as a non-linear hyper-elastic material to estimate the stiffness.

4.2.1. Linear elastic model based stiffness. The MRE inserts in the coupling behave as translational and torsional springs by the rotating axis. This article focuses on the torsional stiffness to calculate the torsional transmissibility.

Using linear elastic model, the torsional stiffness k_T of MRE specimen can be calculated by using the following equation (Hoang et al., 2013)

$$k_T = n \frac{E(\omega)A}{L} r = 6.63 \times 10^{-4} \times E(\omega) [\text{N.m/rad}] \quad (7)$$

where $n = 2$ is the number of MRE specimens, $E(\omega)$ is the dynamic modulus of MRE obtained experimentally in the previous section, A is the specimen area of $7 \times 30 \text{ mm}^2$, L is the length of 46.24 mm, and r is the distance between the MRE specimen and the rotation axis.

Using the model in equation (7), and the elastic modulus data from experiment in the previous section, the dynamic stiffness of the MRE coupling in each frequency under minimum(0 mT), and maximum (150 mT) magnetic flux density can be plotted as shown in Figure 11 and in Table 1.

4.2.2. Non-linear hyper-elastic model-based stiffness. The designed MRE coupling is a complex system which may be treated as a non-linear system. In this case, the MRE is considered as a silicon-based hyper-elastic material which has non-linear relationship between the stress and strain.

The properties of a hyper-elastic material can be explained by using the strain energy density function. There are several models of the strain energy density function to show the behavior of a hyper-elastic material. This study applied the 2-parameter Mooney-Rivlin model, which is the most commonly used non-linear

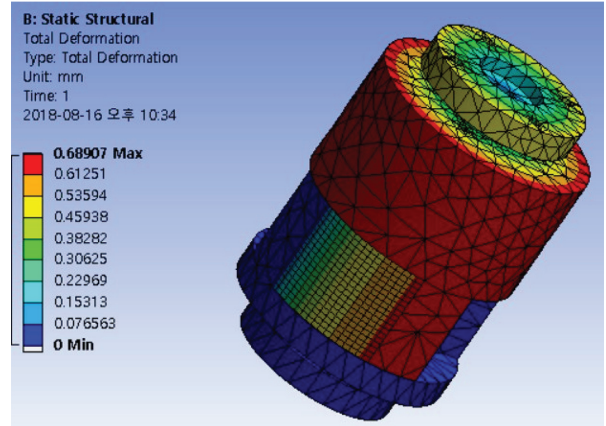


Figure 12. FEM simulation (structural analysis) of torsional stiffness of MRE coupling.

models of the strain energy density. The strain energy density function U is expressed as (Bower, 2009)

$$U = C_{10}(I_1 - 3) + C_{01}(I_2 - 3) + \frac{1}{d}(J - 1)^2 \quad (8)$$

where C_{10} and C_{01} are the Mooney–Rivlin constants, I_1 , I_2 , and I_3 are the strain invariants, d is the incompressibility parameter, and J is the ratio of deformed elastic value.

Assuming that the MRE is soft and the Poisson's ratio is close to 0.5, the Mooney–Rivlin constants (C_{10} , C_{01}) have relationship with elastic modulus as follows (McNamara, 2011)

$$C_{01} = 0.25C_{10}, \quad C_{10} = \frac{E(\omega)}{7.5} \quad (9)$$

The strain invariants (I_1 , I_2 , I_3) are expressed with eigenvalues of principle stretch(λ_i) as

$$\begin{aligned} I_1 &= \lambda_1^2 + \lambda_2^2 + \lambda_3^2 \\ I_2 &= \lambda_1^2 \lambda_2^2 + \lambda_2^2 \lambda_3^2 + \lambda_3^2 \lambda_1^2 \\ I_3 &= \lambda_1^2 \lambda_2^2 \lambda_3^2 \end{aligned} \quad (10)$$

Since the MRE can be assumed to be incompressible, the third term of equation (8) is eliminated by $I_3 = J^2 = 1$

Using the measured modulus values in the previous section, the Mooney–Rivlin constants for each magnetic flux density and frequency can be obtained.

The obtained strain energy (U) is inserted to the property values in the finite element method software (ANSYS) to build the non-linear model of MRE and estimate the stiffness. The non-linear stiffness modeling parameters are summarized in Table 1. The finite element model of the MRE coupling is as shown in Figure 12. In the simulation, torsional displacement is applied as the input and the torsional stiffness of the coupling is calculated. The simulation results of the stiffness with frequency of 1, 10, 20, 30, 40, and 50 Hz,

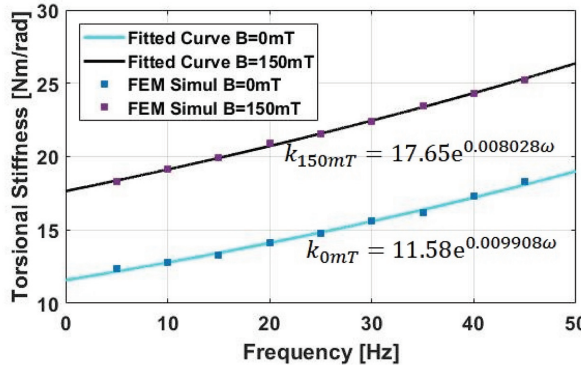


Figure 13. FEM simulation results for torsional stiffness of MRE coupling.

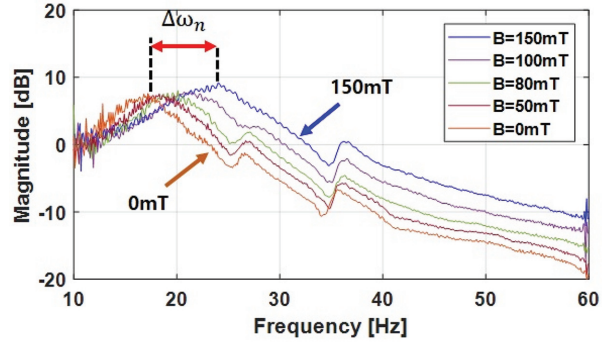


Figure 15. Frequency responses of the MRE coupling at different magnetic fields. It can vary of the stiffness from 20.06 to 39.24 [Nm/rad] under 150 mT.

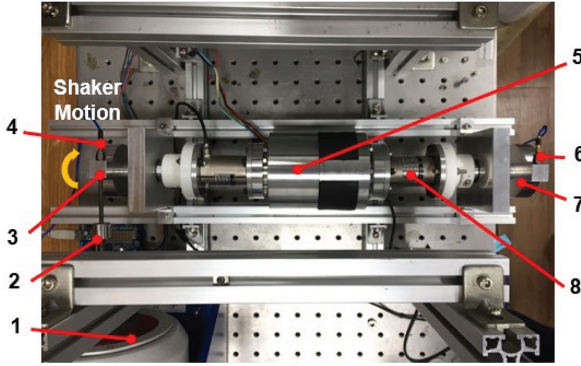


Figure 14. Experimental setup for MRE coupling performance test 1: modal shaker, 2: stinger, 3: input load, 4: accelerometer 1, 5: MRE coupling, 6: accelerometer 2, 7: output load, 8: torque sensor.

under magnetic fields of 0 mT and 150 mT are plotted in Figure 13. The best fit model is obtained to estimate the stiffness of the MRE coupling under 0 mT and 150 mT.

5. Experiment

This section describes experiments to validate the stiffness variation and adaptive vibration suppression performance of the proposed MRE coupling. Also, the comparison between the simulation model of MRE stiffness and experiment results is analyzed.

The torsional vibration response of the proposed system are conducted to obtain the experimental results of stiffness tuning and vibration suppression performance. The experimental setup is shown in Figure 14. The input and output load shafts are connected by the proposed MRE coupling. The source vibration is excited by connecting a modal shaker to the input shaft and is transmitted to the output load shaft via the MRE coupling. The torsional transmissibility between the shafts is measured using accelerometers attached on the input

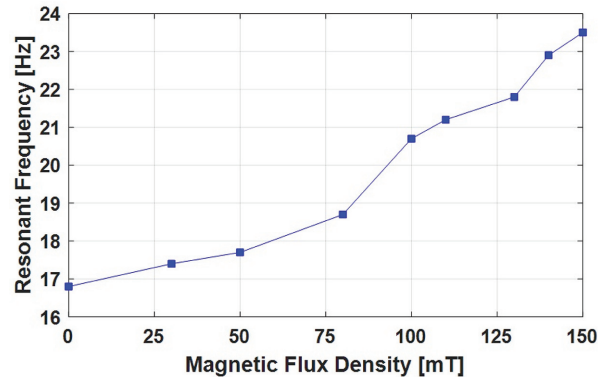


Figure 16. Variation of the resonant frequency under different magnetic field.

and output loads. Experiments are repeated under various magnetic field density which is controlled by the proposed magnetic field generator inside the coupling hubs.

5.1. Frequency response and stiffness tuning range

Modal tests are conducted to obtain the tuning range of the MRE coupling from the system frequency response function under various magnetic field. The input load is excited using the modal shaker with sinusoidal sign sweep at a range of frequencies from 0.1 to 100 Hz. Modal tests are conducted under 10 different magnetic field from 0 mT to 150 mT and some of the results are plotted in Figure 15. Results show that the frequency response is 1-DOF system and the resonance peak shifted to the right from 16.8 to 23.5 Hz, under the magnetic field of 150 mT as shown in Figure 16. The stiffness is shown to be variable in the range of 20.06 to 39.24 [Nm/rad], which is about 96% of MR effect, under 150 mT.

Frequency response function based on simulation stiffness model and experiment results are compared in

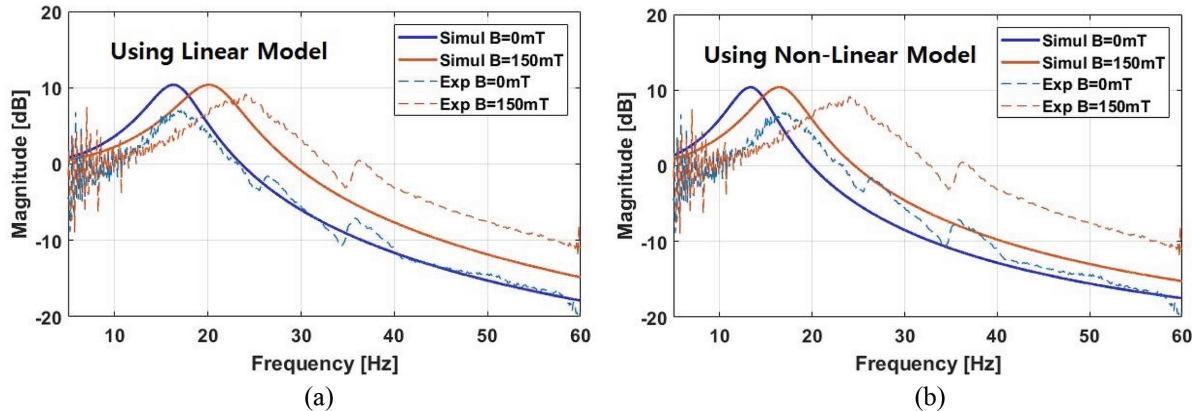


Figure 17. Torsional vibration responses comparison between simulation and experimental results. (a) Simulation result (linear model) vs experimental result; (b) simulation result (non-linear model) vs experimental result.

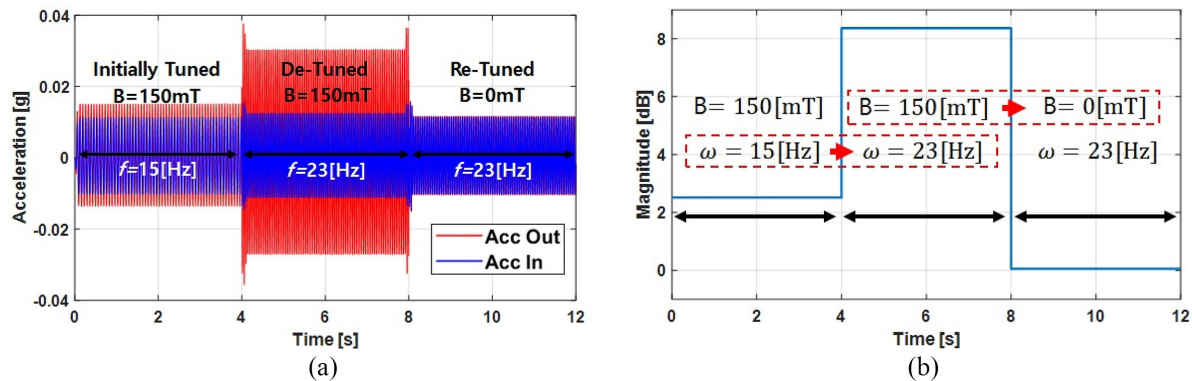


Figure 18. Experimental result of the re-tuning performance. (a) Acceleration in time-domain; (b) variation of transmissibility.

Figure 17(a) and (b). The simulation model in Figure 17(a) is based on the estimated MRE stiffness by using a linear spring model of equation (7), whereas the simulation model in Figure 17(b) is based on Mooney–Rivlin non-linear model for hyper-elastic material. The comparison shows that the simulation that treats the MRE specimen as a linear translational spring is more closely related to the experiment results. The deviations of the linear model simulation could be due to the assumption of the MRE as a rectangular specimen instead of cylindrical.

Although the non-linear modeling of MRE stiffness was studied for the MRE coupling design, which is non-linear system with complex shapes of MRE, it produced more errors. Calculating the Mooney–Rivlin constants using only the Young's modulus that obtained from experimentally may have generated errors that affect the estimation of the non-linear stress-strain curves of the MRE. Also, both simulations showed some deviation from the experiment results. One reason is that the simulation assumed the MRE as a perfect isotropic material with CIP chains, while the actual MRE is not.

5.2. Adaptive vibration reduction performance

The experiment of re-tuning the MRE coupling stiffness for minimum vibration reducing against frequency varying disturbances was conducted. Initially, the MRE coupling is tuned for suppressing vibration of 15 Hz by applying 150 mT, as shown in Figure 18(a). At this state, the magnitude of the transmissibility is measured to be 2.51 dB as shown in Figure 18(b).

When the excitation disturbance is changed from 15 to 23 Hz, without changing the MRE stiffness, the torsional transmissibility increased from 2.51 to 8.37 dB. The magnification of the vibration in time domain during the de-tuned state can be clearly seen in Figure 18(a).

When the MRE coupling is controlled to be in the re-tuned state, by applying the magnetic flux density of 0 mT, the magnitude of the output vibration is reduced to almost 0 dB, as shown in Figure 18(a). By controlling the magnetic field inside the coupling, it can shift the frequency response of the system adaptively to tune the MRE coupling to minimize the frequency changing disturbances.

Table I. System modeling parameters (16.8f<23.5Hz).

Parameter	Symbol	Value (Linear spring model)	Value (FEM)
Output rotational inertia	J_o	0.0018 kg m ²	0.0018 kg m ²
Coupling stiffness	K_{MRE}	23.34 to 36.38 Nm/rad	13.68 to 21.31 Nm/rad
Coupling damping coefficient	C_{MRE}	0.0658 to 0.0821 Nm/rad	0.0504 to 0.0629 Nm/rad
System damping ratio	ζ	0.1605 (const)	0.1605 (const)

FEM: finite element method.

6. Conclusion

This article proposed a novel design of MRE flexible coupling for torsional vibration control. The proposed design is compact in size and possesses an embedded magnetic field generator that allows easy installation on an existing low-frequency power train system, without any complex additional setup or space. The MRE coupling was designed based on simulations using FEM, and the dynamic stiffness of the MRE coupling was estimated by using both linear and non-linear elastic model. Through experiments, it is shown that the proposed MRE coupling exhibits a stiffness tuning of 95.66% and can shift the resonant frequency from 16.8 to 23.5 Hz. The performance of torsional vibration reduction adaptively to varying disturbances by controlling the MRE coupling stiffness was validated with experiment. Experiment results have validated the feasibility of the proposed smart coupling system for the application on an actual power-train system. Since the maximum magnetic field it can generate has a trade-off relationship with the overall dimension, there should be a further study to find the optimal dimension for the required magnetic field.

Declaration of conflicting interests

The author(s) declared no potential conflicts of interest with respect to the research, authorship, and/or publication of this article.

Funding

The author(s) disclosed receipt of the following financial support for the research, authorship, and/or publication of this article: This work was supported by a National Research Foundation of Korea (NRF) grant funded by the Korean government (MSIP) 2016R1C1B1012219. This work was also partially supported by the Korea Hydro&Nuclear Power Company (KHNP) through the Haeoreum Alliance University R&D Cooperation Project No. 20180061.

ORCID iD

Young-Keun Kim  <https://orcid.org/0000-0002-5373-1128>

References

- Bai J, Wu X, Gao F, et al. (2017) Analysis of powertrain loading dynamic characteristics and the effects on fatigue damage. *Applied Sciences* 7: 101027.
- Bower AF (2009) *Applied Mechanics of Solids*. Boca Raton, FL: CRC Press.
- Carlson JD and Jolly MR (2000) MR fluid, foam and elastomer devices. *Mechatronics* 10(4–5): 555–569.
- Deng HX, Gong XL and Wang LH (2006) Development of an adaptive tuned vibration absorber with magnetorheological elastomer. *Smart Materials and Structures* 15: N111.
- DeSmidt HA, Wang K and Smith EC (2002) Coupled torsion-lateral stability of a shaft-disk system driven through a universal joint. *Journal of Applied Mechanics* 69(3): 261–273.
- Drexel HJ (1987) Torsional dampers and alternative systems to reduce driveline vibrations. *SAE Transactions* 96: 78–88.
- Hashi HA, Muthalif AG and Nordin ND (2016) Dynamic tuning of torsional transmissibility using magnetorheological elastomer: modelling and experimental verification. *Iranian Journal of Science and Technology, Transactions of Mechanical Engineering* 40(3): 181–187.
- Hoang N, Zhang N and Du H (2009) A dynamic absorber with a soft magnetorheological elastomer for powertrain vibration suppression. *Smart Materials and Structures* 18: 7074009.
- Hoang N, Zhang N and Du H (2010) An adaptive tunable vibration absorber using a new magnetorheological elastomer for vehicular powertrain transient vibration reduction. *Smart Materials and Structures* 20: 1015019.
- Hoang N, Zhang N, Li W, et al. (2013) Development of a torsional dynamic absorber using a magnetorheological elastomer for vibration reduction of a powertrain test rig. *Journal of Intelligent Material Systems and Structures* 24(16): 2036–2044.
- Hwang SJ, Chen JS, Liu L, et al. (2000) Modeling and simulation of a powertrain-vehicle system with automatic transmission. *International Journal of Vehicle Design* 23(1–2): 145–160.
- Jang DI, Yun GE, Park JE, et al. (2018) Designing an attachable and power-efficient all-in-one module of tunable vibration absorber based on magnetorheological elastomer. *Smart Materials and Structures* 27: 085009.
- Kim HK, Kim HS and Kim YK (2017) Stiffness control of magnetorheological gels for adaptive tunable vibration absorber. *Smart Materials and Structures* 26(1): 015016.

- Kim J (2005) Launching performance analysis of a continuously variable transmission vehicle with different torsional couplings. *Journal of Mechanical Design* 127(2): 295–301.
- Kim YK, Bae HI, Koo JH, et al. (2012) Note: real time control of a tunable vibration absorber based on magnetorheological elastomer for suppressing tonal vibrations. *Review of Scientific Instruments* 83(4): 046108.
- Kim YK, Koo J, Kim KS, et al. (2011) Suppressing harmonic vibrations of a miniature cryogenic cooler using an adaptive tunable vibration absorber based on magnetorheological elastomers. *Review of Scientific Instruments* 82: 3035103.
- Li Y, Li J, Li W, et al. (2013) Development and characterization of a magnetorheological elastomer based adaptive seismic isolator. *Smart Materials and Structures* 22: 3035005.
- McNamara J (2011) Novel approaches to the analysis of localised stress concentrations in deformed elastomers. Available at: <https://arrow.dit.ie/cgi/viewcontent.cgi?article=1045&context=engdoc>
- Shin BC, Yoon JH, Kim YK, et al. (2015) Note: vibration suppression using tunable vibration absorber based on stiffness variable magneto-rheological gel. *Review of Scientific Instruments* 86(10): 106106.
- Steinel K and Tebbe G (2004) New torsional damper concept to reduce idle rattle in truck transmissions. SAE technical paper 2004-01-2722.
- Stepanov G, Abramchuk S, Grishin D, et al. (2007) Effect of a homogeneous magnetic field on the viscoelastic behavior of magnetic elastomers. *Polymer* 48(2): 488–495.
- Sun S, Yang J, Li W, et al. (2017) Development of an isolator working with magnetorheological elastomers and fluids. *Mechanical Systems and Signal Processing* 83: 371–384.
- Xin FL, Bai XX and Qian LJ (2017) Principle, modeling, and control of a magnetorheological elastomer dynamic vibration absorber for powertrain mount systems of automobiles. *Journal of Intelligent Material Systems and Structures* 28(16): 2239–2254.
- Xu M and Marangoni R (1994) Vibration analysis of a motor-flexible coupling-rotor system subject to misalignment and unbalance, part i: theoretical model and analysis. *Journal of Sound and Vibration* 176(5): 663–679.
- Yamauchi T, Yamazaki Y and Kimura J (1999) Experiment and computation analyses for torsional vibration of crank-shaft system with viscous torsional damper on diesel engine. SAE technical paper 1999-01-1748.
- Yang J, Sun S, Du H, et al. (2014) A novel magnetorheological elastomer isolator with negative changing stiffness for vibration reduction. *Smart Materials and Structures* 23(10): 105023.
- Yang J, Sun S, Tian T, et al. (2016) Development of a novel multi-layer MRE isolator for suppression of building vibrations under seismic events. *Mechanical Systems and Signal Processing* 70: 811–820.
- Zhang N, Crowther A, Liu D, et al. (2003) A finite element method for the dynamic analysis of automatic transmission gear shifting with a four-degree-of-freedom planetary gearset element. *Proceedings of the Institution of Mechanical Engineers, Part D: Journal of Automobile Engineering* 217(6): 461–473.
- Zhou G (2003) Shear properties of a magnetorheological elastomer. *Smart Materials and Structures* 12(1): 139.